Crystal Structure and Its Role in Electrical Properties of the Perovskite $CaPbO_3$ Synthesized at High Pressure

A. Yamamoto,*,† N. R. Khasanova,† F. Izumi,‡ X.-J. Wu,† T. Kamiyama,§ S. Torii,§ and S. Tajima†

Superconductivity Research Laboratory, International Superconductivity Technology Center, 1−10−13 Shinonome, Koto-ku, Tokyo 135-0062, Japan, National Institute for Research in Inorganic Materials, 1−1 Namiki, Tsukuba-shi, Ibaraki 305-0044, Japan, and Institute of Materials Science, University of Tsukuba, Tennodai, Tsukuba-shi, Ibaraki 305-8573, Japan

Received September 11, 1998. Revised Manuscript Received November 9, 1998

The orthorhombic modification of $CaPbO_3$ was synthesized from a mixture of Ca_2PbO_4 and PbO_2 at high temperature and high pressure. Its structure was analyzed by Rietveld analysis of neutron diffraction data on the basis of space group Pbnm. It has a distorted perovskite structure of the $GdFeO_3$ type and a unit cell with dimensions of $a = 5.6710$ Å, $b = 5.8875$ Å, and $c = 8.1495$ Å. The Pb−O bond lengths in each PbO_6 octahedron are comparable to each other, whereas the PbO_6 octahedron tilts around $[110]_p$ and $[001]_p$ axes (p: perovskite subcell) by 18.50° and 20.28°, respectively. These tilt angles, which show great structural distortion in $CaPbO_3$ containing the smaller Ca^{2+} ion, are much larger than corresponding ones in crystal chemically isotypic $SrPbO_3$. The electric resistivity of $CaPbO_3$ at room temperature was as high as 3×10^3 Ω•cm, which is in sharp contrast to low resistivities observed in other perovskite-type oxides $BaPbO_3$ and $SrPbO_3$. The high resistivity of $CaPbO_3$ is explained as gap formation between 2p(O) nonbonding and 6s(Pb)-2p(O) spσ antibonding bands, which overlap with each other in $BaPbO_3$. Solid solutions, where Sr^{2+}, La^{3+}, Nd^{3+}, and Y^{3+} ions were partially substituted for Ca^{2+} ions, were also prepared to examine structural and electrical properties in perovskites based on $CaPbO_3$. Substitution of Sr^{2+} for Ca^{2+} led to reductions in the distortion and gap energy, whereas that of La^{3+}, Nd^{3+}, and Y^{3+} induced metallic conductivity owing to doping of electron carriers into the antibonding band.

Introduction

In recent years, structural and electronic properties of barium/strontium lead(IV) oxides with perovskite-related layer and/or network structures containing PbO_6 octahedra have been extensively studied with the intention of synthesizing copper-free superconducting oxides.[1−7] $BaPbO_3$, with space group Ibmm,[5] is a metallic conductor and the mother phase of superconducting $Ba(Pb_{1-x}Bi_x)O_3$.[8] $BaPbO_3$ owes its high conductivity to overlapping of the 2p(O) nonbonding band with the 6s(Pb)-2p(O) spσ antibonding band at the Fermi level.[9] The degree of overlapping of the two bands is believed to decrease in $SrPbO_3$ with a $GdFeO_3$-type structure (space group Pbnm),[5,10] but this oxide still exhibits metallic behavior in conductivity[7] and thermoelectric power.[11] It remains open whether the metallic conductivity in $SrPbO_3$ arises from the overlap of the two bands despite its decrease in comparison with $BaPbO_3$ or from electron doping due to oxygen nonstoichiometry in the absence of any band overlap.[7] Thus, these lead(IV) oxides are of great interest in connection with their low-carrier electric conductivity closely associated with a three-dimensional network of PbO_6 octahedra sharing corners.

For systematic investigation of the effects of alkaline earth metals at A sites cations on the electrical and structural properties of $APbO_3$, perovskite-type $CaPbO_3$ containing smaller Ca^{2+} ions needs to be obtained in addition to $BaPbO_3$ and $SrPbO_3$. A tolerance factor of 0.89 estimated for $CaPbO_3$ appears to be large enough for a distorted perovskite to occur. However, perovskite-type $CaPbO_3$ was never formed on heating metal oxides or carbonates above 600 °C at ambient pressure because

* To whom correspondence should be addressed. Telephone: +81-3-3536-0618. FAX: +81-3-3536-5714. E-mail: yamamoto@istec.or.jp.
† Superconductivity Research Laboratory.
‡ National Institute for Research in Inorganic Materials.
§ University of Tsukuba.

(1) Itoh, M.; Sawada, T.; Kim, I.-S.; Imaguma, Y.; Nakamura, T. *Solid State Commun.* **1992**, *83*, 33.
(2) Cava, R. J.; Takagi, H.; Karajewski, J. J.; Peck, W. F., Jr.; Hwang, H. Y. *Phys. Rev. B* **1993**, *47*, 11525.
(3) Fu, W. T.; Zandbergen, H. W.; Xu, Q.; van Ruitenbeek, J. M.; de Jongh, L. J.; van Tendeloo, G. *Solid State Commun.* **1989**, *70*, 1117.
(4) Cava, R. J.; Takagi, H.; Zandbergen, H. W.; Hessen, B.; Karajewski, J. J.; Peck, W. F., Jr. *Phys. Rev. B* **1993**, *47*, 11525.
(5) Fu, W. T.; Ijdo, D. J. W. *Solid State Commun.* **1995**, *95*, 581.
(6) Mattheiss, L. F. *Phys. Rev. B* **1990**, *42*, 359.
(7) Lobanov, M. V.; Kopnin, E. M.; Xenikos, D.; Grippa, A. Ju.; Antipov, E. V.; Capponi, J. J.; Marezio, M.; Julien, J. P.; Tholence, J. L. *Mater. Res. Bull.* **1997**, *32*, 983.
(8) Sleight, A. W.; Gllson, J. L.; Bierstedt, P. E. *Solid State Commun.* **1975**, *17*, 27.
(9) Mattheiss, L. F.; Hamann, D. R. *Phys. Rev. B* **1983**, *28*, 4227.
(10) Keller, H. L.; Meier, K. H.; Müller-Buschbaum, Hk. *Z. Naturforsch., B* **1975**, *30*, 277.
(11) Yamamoto, A.; Ono, T. In *High-Temperature Superconductors and Novel Inorganic Materials*; van Tendeloo, G. et al., Eds.; Kluwer Academic Publishers: The Netherlands, 1990; p 123.

10.1021/cm980629p CCC: $18.00
Published on Web 02/24/1999

of the formation of Ca_2PbO_4. Another modification of $CaPbO_3$, which resulted from thermal decomposition of $CaPb(OH)_6$ at low temperatures between 400 and 500 °C, crystallized in trigonal form with an ilmenite-type structure.[12,13]

We have recently succeeded in preparing perovskite-type $CaPbO_3$ at high temperature and high pressure.[14] In the present work, we have optimized synthetic conditions for synthesizing $CaPbO_3$ of high purity and investigated its structural, physical, and chemical properties in detail. The structure refinement of $CaPbO_3$ by neutron diffraction has enabled us to reveal the relationship between the crystal structure and electric conductivity unambiguously. We have further prepared several solid solutions based on $CaPbO_3$ to attain metallic conductivity.

Experimental Section

Materials. Our previous work[14] showed that reacting CaO with PbO_2 at high pressure afforded $CaPbO_3$ with accompanying formation of small amounts of $Ca(OH)_2$ and others. During the course of efforts to improve the purity of products, we had an opportunity to develop a better synthetic route from Ca_2PbO_4 to $CaPbO_3$. The Ca_2PbO_4 precursor was prepared by calcining a mixture of $CaCO_3$ (99.99%) and PbO_2 (99.99%) at 850 °C in air. Various samples of $CaPbO_3$ were synthesized from a mixture of Ca_2PbO_4 and PbO_2 with addition of PbO (99.9%) at need to change nominal oxygen contents. About 150 mg of the mixtures were pressed into a cylindrical shape, charged in gold capsules, and then heated at 900−1200 °C and 3−6.5 GPa for 1−3 h using a cubic-anvil-type apparatus (TRY Engineering, 700-ton press). $Ca_{1-x}Sr_xPbO_3$ and $Ca_{1-x}R_xPbO_3$ (R = La, Nd and Y) were produced in a similar manner by adding SrO_2 (99%) and R_2O_3 (99.99%) dried at 140 °C and 950 °C in air, respectively. We also attempted to synthesize $CdPbO_3$ either from CdO (99.9%) dried at 900 °C or from Cd_2PbO_4 and PbO_2 under 5−6.5 GPa.

Lattice parameters in several samples made with the 700-ton press were slightly different from each other despite the same synthetic conditions. Accordingly, a specimen for a neutron powder diffraction experiment was prepared with another cubic-anvil-type apparatus (TRY Engineering, 1200-ton press) by heating the starting mixture at 1000 °C and 5 GPa for 1 h. The use of the 1200-ton press made it possible to get ≈800 mg of the product in one experiment. The resultant sample included a small amount of Ca_2PbO_4, most probably due to temperature inhomogeneity in a gold capsule with a difference of ≈100 °C between the center and edge of the sintered block.

Characterization. The samples were identified by X-ray powder diffraction (XRD) with CuKα radiation on a Mac Science MXP18 diffractometer. Their lattice parameters were refined with their XRD data by the least-squares method. Electron diffraction patterns were taken on a JEM-2010 F analytical transmission electron microscope operated at an accelerating voltage of 200 kV and equipped with a side-entry double-tilt goniometer with maximum tilt angles of ±42° around the *x* axis and ±30° around the *y* axis. Crystal-structure images were observed with a JEM-4000 EX high-resolution transmission electron microscope operated at an accelerating voltage of 400 kV.

Metal contents in the product with a nominal composition of $CaPbO_3$ were determined by energy-dispersive X-ray (EDX) analysis using the ZAF method at 15 different points on a JSM-840 scanning electron microscope (SEM) with an accelerating voltage of 25 kV. Metal contents were also analyzed by inductively coupled plasma (ICP) emission spectrometry after dissolving it in 1 mol/dm^3 nitric acid. An oxygen content was determined by the iodometric-titration method with a Metrohm auto-titrator.

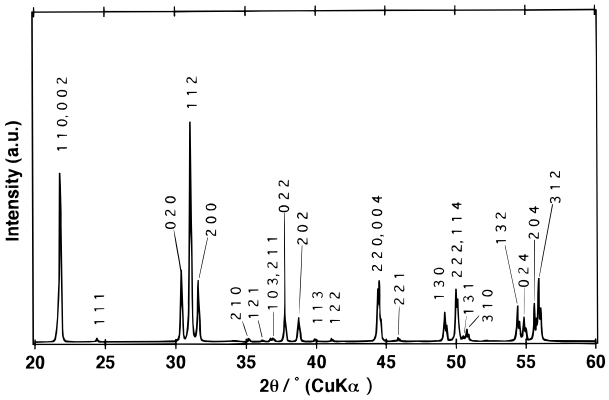

Figure 1. XRD pattern of perovskite-type $CaPbO_3$.

Neutron Powder Diffraction. Time-of-flight neutron powder diffraction data for $CaPbO_3$ were measured at room temperature for ≈2 d on the Vega diffractometer[15] at the KENS pulsed neutron scattering facility. A cylindrical block of the specimen (567 mg in weight, 4.0 mm in diameter, and 6.9 mm in height) was supported in the neutron beam using an Al foil (2.7 mg). The foil was partly covered with a Cd plate, 0.5 mm in thickness, to reduce unnecessary scattering of neutrons. The specimen was rotated during data acquisition. The resulting diffraction pattern contained weak reflections due to Ca_2PbO_4 (impurity) and Cd (shielding material).

Measurements. Thermogravimetric analyses (TGA) were carried out using a Perkin-Elmer System 7 with pulverized samples. The samples (20 mg) were heated and then cooled at a rate of 5 °C/min in a 1 atm O_2 gas flowing at a rate of 50 cm^3/min. Electric resistivities were measured by the conventional four-probe method using sintered samples.

Results and Discussion

Characterization of the Products and Phase Studies of the System. $Ca_{1-x}Pb_{1+x}O_{3-\delta}$. The use of Ca_2PbO_4 and PbO_2 as the starting materials yielded single-phase samples. Impurities could not be detected by XRD in any significant amount in samples sintered at 1000−1100 °C and 5 GPa for 1 h, whereas a small amount of $Ca(OH)_2$ was contained when CaO and PbO_2 were used as starting materials.[14] Sintering below 900 °C or above 1200 °C led to the formation of traces of impurities such as Ca_2PbO_4. We also changed pressure (3−6.5 GPa) and reaction time (1−3 h), but found no appreciable change in terms of product.

Figures 1 and 2 give an XRD and electron diffraction patterns of $CaPbO_3$, respectively. All the reflections in these patterns could be indexed on the basis of an orthorhombic unit cell with $a = 5.661(1)$ Å $\approx\sqrt{2}a_p$, $b = 5.878(1)$ Å $\approx\sqrt{2}a_p$, and $c = 8.136(1)$ Å $\approx\sqrt{2}a_p$, where subscript p denotes the lattice parameter of the cubic perovskite-type compound. Table 1 lists reflection indices, observed and calculated lattice-plane spacings, *d*, and relative intensities in the XRD pattern. Reflection conditions determined from the XRD and electron diffraction patterns were $h + l = 2n$ for $h0l$, $k = 2n$ for $0kl$, $h = 2n$ for $h00$, $k = 2n$ for $0k0$ and $l = 2n$ for $00l$,

(12) Levy-Clement, C.; Michel, A. *Ann. Chim. (Paris)* **1975**, *10*, 63.
(13) Levy-Clement, C. *Ann. Chim. (Paris)* **1975**, *10*, 105.
(14) Yamamoto, A.; Khasanova, N. R.; Wu, X.-J.; Tanabe, K. *Solid State Ionics* **1998**, *108*, 333.
(15) Kamiyama, T.; Oikawa, K.; Tsuchiya, N.; Osawa, M.; Asano, H.; Watanabe, N.; Furusaka, M.; Satoh, S.; Fujikawa, I.; Ishigaki, T.; Izumi, F. *Physica B* **1995**, *213−214*, 875.

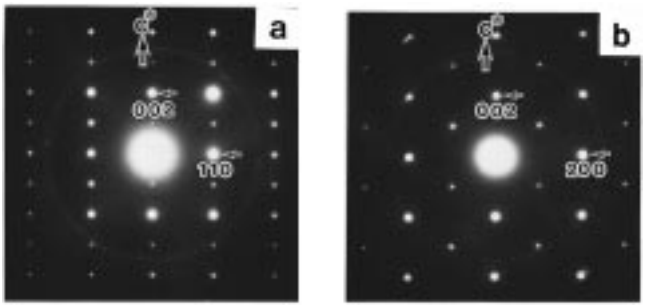

Figure 2. Selected-area electron diffraction patterns of $CaPbO_3$ taken with incident beams parallel to (a) [110] and (b) [010] directions. Double reflections of 00*l* with $l = 2n + 1$ were observed in (a).

Table 1. Observed and Calculated Lattice-Plane Spacings and Relative Intensities, *I*, of $CaPbO_3$[a]

h	*k*	*l*	d_{obs}, Å	d_{cal}, Å	*I*
1	1	0	4.072	4.078	75
0	0	2	4.072	4.068	
1	1	1	3.643	3.646	2
0	2	0	2.939	2.939	33
1	1	2	2.878	2.880	100
2	0	0	2.830	2.831	29
2	1	0	2.550	2.550	2
1	2	1	2.483	2.484	1
1	0	3	2.444	2.446	2
2	1	1	2.433	2.434	2
0	2	2	2.382	3.383	14
2	0	2	2.323	2.324	11
1	1	3	2.258	2.258	1
1	2	2	2.195	2.196	2
2	2	0	2.039	2.039	28
0	0	4	2.034	2.034	21
2	2	1	1.978	1.978	2
1	3	0	1.851	1.852	15
2	2	2	1.823	1.823	28
1	1	4	1.823	1.820	
1	3	1	1.806	1.806	2
3	1	0	1.797	1.797	6
3	1	1	1.754	1.755	1
1	3	2	1.686	1.685	18
0	2	4	1.673	1.673	12
2	0	4	1.652	1.652	19
3	1	2	1.643	1.644	33
2	2	3	1.630	1.630	1
1	3	3	1.530	1.529	1
0	4	0	1.4703	1.4696	2
0	4	1	1.4465	1.4462	1
2	2	4	1.4403	1.4400	10
1	4	0	1.4231	1.4237	1
4	0	0	1.4158	1.4154	5
0	4	2	1.3827	1.3822	9
1	3	4	1.3697	1.3693	5
3	3	0	1.3599	1.3593	5
0	0	6	1.3599	1.3561	
3	1	4	1.3471	1.3467	5
4	0	2	1.3371	1.3368	3
2	4	0	1.3048	1.3043	3
3	3	2	1.2898	1.2892	5
1	1	6	1.2871	1.2868	11
4	2	0	1.2756	1.2752	7
2	4	2	1.2424	1.2420	10
0	2	6	1.2320	1.2320	6
2	0	6	1.2232	1.2230	3
4	2	2	1.2173	1.2168	7

[a] $a = 5.661(1)$ Å, $b = 5.878(1)$ Å, and $c = 8.136(1)$ Å.

revealing possible space groups to be $Pbn2_1$ (standard setting: $Pna2_1$, no. 33) and Pbnm (standard setting: *Pnma*, no. 62). $SrPbO_3$ also crystallizes with space group Pbnm and rather larger lattice parameters.[5,10] The crystal-structure image shown in Figure 3 confirms that

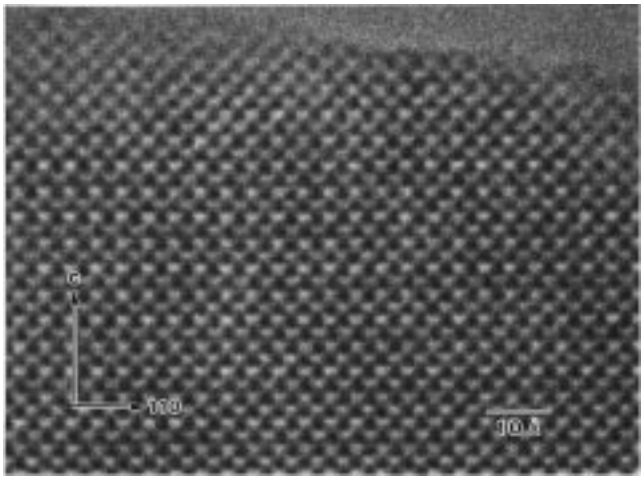

Figure 3. Crystal-structural image of $CaPbO_3$ taken with incident beams parallel to the [110] direction.

Table 2. Lattice Parameters and Unit-Cell Volumes, *V*, of $Ca_{1-x}Pb_{1+x}O_{3-\delta}$

nominal composition	*a*, Å	*b*,' Å	*c*, Å	*V*, Å^3	impurities
$CaPbO_3$	5.661(1)	5.878(1)	8.136(1)	270.7(1)	none
$CaPbO_{2.95}$	5.674(1)	5.887(1)	8.154(2)	272.3(2)	trace
$CaPbO_{2.90}$	5.674(2)	5.889(2)	8.155(3)	272.5(4)	Ca_2PbO_4
$Ca_{0.9}Pb_{1.1}O_{3.0}$	5.676(3)	5.887(2)	8.165(4)	272.8(5)	trace

the atomic arrangement in $CaPbO_3$ is basically consistent with a perovskite-type structure. From the crystallographic information just described, we can conclude that $CaPbO_3$ is isotypic with $SrPbO_3$, having the Gd-FeO_3-type structure.[5,10] The density of perovskite-type $CaPbO_3$ calculated from the above lattice parameters just given is 7.21 g/cm^3. This density is much larger than that of ilmenite-type $CaPbO_3$ (6.86 g/cm^3[3,13]), which is in accord with the general rule that the high-pressure form has a higher density and larger coordination numbers than the low-pressure form.

We further examined the effect of nominal compositions, $CaPbO_{3-\delta}$ and $Ca_{1-x}Pb_{1+x}O_3$, on products to check whether the perovskite-type phase can be crystallized with varying oxygen deficiencies and substitutional defects, respectively. Table 2 lists nominal compositions, lattice parameters, and impurities for products formed by heating at 1000 °C and 5 GPa for 1 h. For all the nominal compositions, perovskite-type $CaPbO_3$ was predominately produced (rough estimate by XRD > 90 mass %) with lattice parameters scattered within some ranges, which implies that the formation of the perovskite phase proceeds nonstoichiometrically. Nevertheless, high-pressure synthesis with variation of nominal compositions presented no clear evidence for the nonstoichiometry in this system because only the stoichiometric nominal composition of $CaPbO_3$ yielded monophasic products. The gold capsule used in our high-pressure synthesis serves as an effective container to prevent the loss of the contents and reduction of Pb^{4+} ions at high temperature. Then, the nominal composition was fixed at the stoichiometric one, viz., $CaPbO_3$, in subsequent syntheses.

SEM-EDX analysis and ICP emission spectrometry showed the ratios of the amount of Ca to that of Pb to be 0.95(4):1.00(4) and 0.97(2):1.00(2), respectively. These analytical values are in good agreement with each other

in view of the standard deviations, indicating no appreciable cation deficiency. The oxygen content of the $CaPbO_3$ sample was found to be 2.95(2) per formula unit by the iodometry. The SEM observations revealed that the grain size of the sample was about 100 μm on average, depending on sintering temperature. Column-like crystallites ≈300 μm in length and ≈50 μm in diameter resulted from sintering at 1200 °C.

Structure Refinement of $CaPbO_3$ by Neutron Powder Diffraction. We refined the structure parameters of $CaPbO_3$ by the Rietveld method with RIETAN-96T[16,17] using 3487 points of intensity data, which included 1211 reflections in a d range between 0.496 and 3.66 Å. Bound coherent scattering lengths, b_c, used for the refinement were 9.4017 fm (Pb), 4.90 fm (Ca), and 5.803 fm (O).[18] Ca_2PbO_4 and Cd were introduced as minor phases into multiphase Rietveld analysis. Structural parameters of Ca_2PbO_4 and Cd were fixed at those described in the literature[19,20] while their scale factors and lattice parameters were refined. Isotropic atomic displacement parameters, B, were assigned to all the sites. An original technique called partial profile relaxation in RIETAN-96T[17] was applied to the 312, 204, 132, 004, 220, 121, 210, and 140 reflections of $CaPbO_3$ in a large d region, which decreased R_{wp} by ≈0.2%.

At first, we compared the results of refinements with noncentrosymmetric $Pbn2_1$ and centrosymmetric Pbnm space groups, assuming the full occupation of all the sites and perfect ordering of Ca and Pb atoms. The Rietveld refinement with $Pbn2_1$, where all the atoms were located at general positions 4a, gave slightly lower R factors than those obtained with Pbnm because of the lowering of symmetry. However, the estimated standard deviations of fractional coordinates and all the B parameters for the $Pbn2_1$ model were much larger than corresponding ones for the Pbnm model. The reasonable B parameters resulting from the refinement with Pbnm imply the absence of any significant positional disorder. These preliminary refinements led us to rule out $Pbn2_1$ and adopt Pbnm, to which $SrPbO_3$ also belongs,[5,10] in subsequent refinements.

Lattice parameters refined with the neutron diffraction data were slightly larger than those obtained with the XRD data. This fact prompted us to check some possible models of defect structures. At first, we tested a structural model assuming partial substitution of Pb for Ca at the 4c site because the composition of the perovskite phase may be slightly Pb rich owing to the concomitant appearance of Ca_2PbO_4; the large difference in b_c between Ca and Pb enables us to obtain their reliable occupancies, g, at the A site. With this disordering model and a linear constraint of $g(\mathrm{Ca}) + g(\mathrm{Pb}) = 1$ for the 4c site, g(Pb) converged on −0.014(2), which suggests ordering of Ca at 4c and Pb at 4a. No detectable amount of deficiencies was found at the Ca site on refinement of g(Ca). Refinement of g(O1) and g(O2) suggested that oxygen deficiencies in $CaPbO_3$ are negligible, if any. Thus, these preliminary refinements did not offer any evidence for the existence of vacancies or substitutional defects. In the final refinement, we adopted the stoichiometric structural model where every site is fully occupied by one chemical species.

Table 3. Final Results of the Rietveld Refinement with the Neutron Diffraction Data for $CaPbO_3$[a]

atom	site	g	x	y	z	B, Å^2
Ca	4c	1	0.9860(3)	0.0563(2)	1/4	0.84(3)
Pb	4a	1	1/2	0	0	0.38(2)
O1	4c	1	0.1200(3)	0.4452(2)	1/4	0.67(3)
O2	8d	1	0.6907(2)	0.3051(2)	0.0613(2)	0.96(2)

[a] $Z = 4$; space group Pbnm (no. 62); $a = 5.67102(4)$ Å, $b = 5.88752(4)$ Å, and $c = 8.14954(6)$ Å; $V = 272.099(4)$ Å^3.

Table 4. Selected Interatomic Distances (Å) and Bond Angles (degree) in $CaPbO_3$ and $SrPbO_3$[a]

bond	$CaPbO_3$	$SrPbO_3$[b]
Pb−O2	2.155(1) ×2	2.165(1) ×2
Pb−O2^{i}	2.155(1) ×2	2.157(1) ×2
Pb−O1^{ii}	2.1721(5) ×2	2.1573(7) ×2
Ca/Sr−O1^{i}	2.328(2)	2.498(4)
Ca/Sr−O2^{i}	2.358(2) ×2	2.510(2) ×2
Ca/Sr−O1^{iii}	2.412(2)	2.602(2)
Ca/Sr−O2	2.705(2) ×2	2.821(2) ×2
Ca/Sr−O2^{ii}	2.907(2) ×2	2.933(2) ×2
O1^{ii}−Pb−O2^{i}	92.39(5)	91.43(9)
O1^{iv}−Pb−O2	93.65(5)	91.76(8)
O2−Pb−O2^{v}	91.05(2)	90.99(2)

[a] Symmetry codes: (i) $-x + 3/2, y - 1/2, z$; (ii) $x + 1/2, -y + 1/2, -z$; (iii) $x - 1, y, z$; (iv) $-x + 1/2, y - 1/2, z$; (v) $x - 1/2, -y + 1/2, -z$. [b] Taken from ref 5.

Table 3 lists the final structural parameters of $CaPbO_3$. Metal−oxygen interatomic distances, l, and bond angles in $CaPbO_3$ calculated with ORFFE[21] are given in Table 4, together with those in $SrPbO_3$[5] for reference. Figure 4 shows observed, calculated, and difference patterns for $CaPbO_3$ plotted as a function of d. The R factors were $R_{wp} = 4.92\%$ and $R_p = 3.73\%$ for the observed and calculated patterns, and $R_B = 1.05\%$ and $R_F = 1.18\%$ for $CaPbO_3$. The mass percentages of $CaPbO_3$ and Ca_2PbO_4 in the sample were 93% and 7%, respectively.

Our structure refinement unequivocally revealed that perovskite-type $CaPbO_3$ is crystal chemically isotypic to $SrPbO_3$[5,10] as well as $CaMO_3$ where M = Ti,[22] Mn,[23] Zr,[24] and Hf.[25] The $GdFeO_3$-type compound, whose structure suffers distortion from the ideal cubic perovskite structure, is characterized by 8-fold coordination of the A-site cation and nearly regular BO_6 octahedra tilted with each other. Figure 5 displays the crystal structure of $CaPbO_3$ in a couple of ways. As illustrated by broken lines in Figure 5a, every Ca^{2+} ion is surrounded by eight oxide ions with Ca−O bond lengths ranging from 2.498 to 2.907 Å. Each Pb^{4+} ion is

(16) Izumi, F. In *The Rietveld Method*; Young, R. A., Ed.; Oxford University Press: Oxford, 1995; Chapter 13.
(17) Ohta, T.; Izumi, F.; Oikawa, K.; Kamiyama, T. *Physica B* **1997**, *234*, 1093.
(18) Sears, V. F. In *International Tables for Crystallography*; Wilson, A. J. C., Ed.; Kluwer: Dordrecht, 1992; Vol. C, pp 383−391.
(19) Teichert, A.; Müller-Buschbaum, Hk. *Z. Anorg. Allg. Chem.* **1992**, *607*, 128.
(20) Wells, A. F. In *Structural Inorganic Chemistry*; Clarendon Press: Oxford, 1984; p 1277.
(21) Busing, W. R.; Martin, K. O.; Levy, H. A. *ORFFE*, Report ORNL-TM-306; Oak Ridge National Laboratory: Tennessee, 1964.
(22) Sasaki, S.; Prewitt, C. T.; Bass, J. D. *Acta Crystallogr.* **1987**, *43C*, 1668.
(23) Poeppelmeier, K. R.; Leonowicz, M. E.; Scanlon, J. C.; Longo, J. M.; Yelon, W. B. *J. Solid State Chem.* **1982**, *45*, 71.
(24) Koopmanns, H. J. A.; van de Valde, G. M. H.; Gellings, P. J. *Acta Crystallogr.* **1983**, *39C*, 1323.
(25) McMurdie, H.; Morris, M.; Evans. E.; Paretzkin, B.; Wong-Ng, W.; Hubbard, C. *Powder Diffr.* **1986**, *1*, 87.

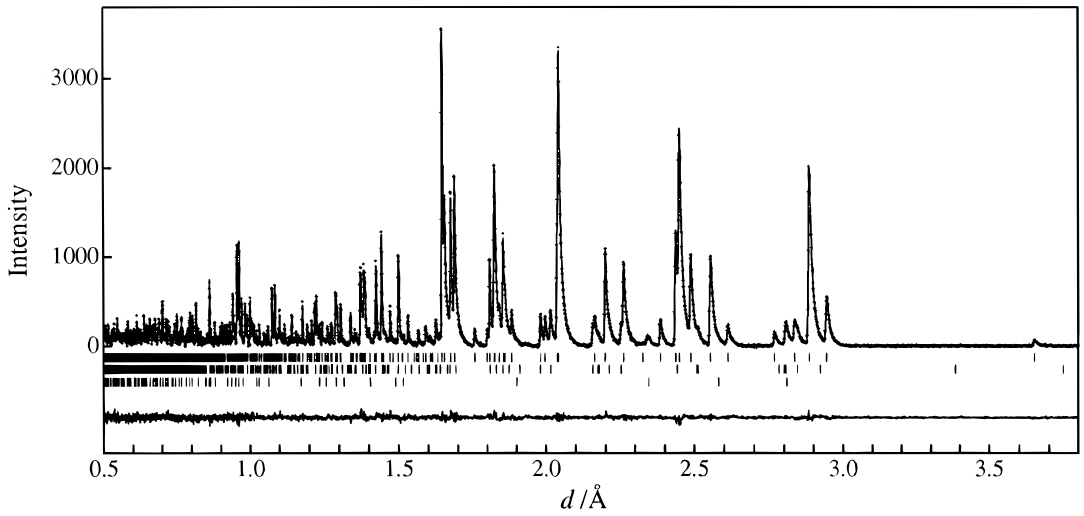

Figure 4. Rietveld-refinement patterns for $CaPbO_3$. Plus (+) symbols represent the observed diffraction data, which are overlapped by a calculated pattern (solid line). The tick marks below the diffraction patterns denote the positions of possible Bragg reflections for $CaPbO_3$ (top), Ca_2PbO_4 (middle), and Cd (bottom). Differences between observed and calculated intensities are plotted at the bottom.

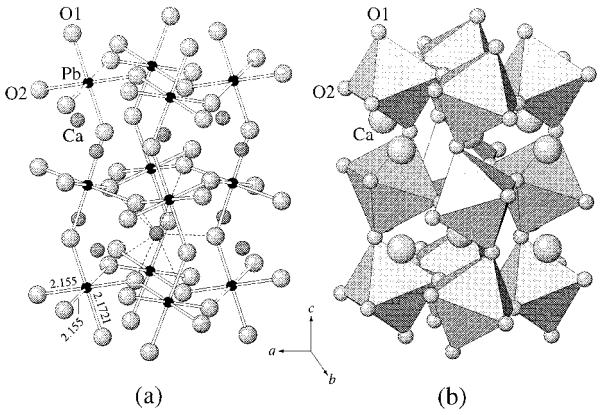

Figure 5. Crystal structure of $CaPbO_3$ represented with (a) a ball-and-stick model and (b) PbO_6 octahedra with oxygen atoms at corners. In (a), Pb and O atoms are connected with bonds. Eight Ca−O bonds are shown with broken lines for only one Ca atom, for convenience. Numbers attached to three Pb−O bonds denote their lengths (Å). Note that the sizes of Ca and O atoms in (a) and (b) are different from each other.

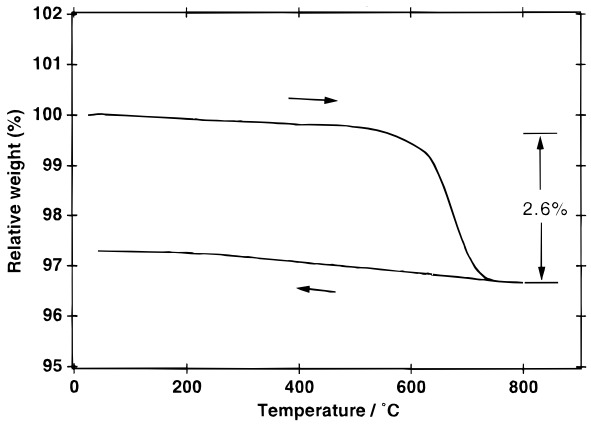

Figure 6. Dependence of relative weight for $CaPbO_3$ on temperature during heating and subsequent cooling processes in an atmosphere of flowing O_2.

octahedrally coordinated to six oxide ions. The PbO_6 octahedron is quite regular with comparable Pb−O bond lengths: 2.155 Å (×2), 2.155 Å (×2), and 2.172 Å (×2) as noted in Figure 5a. The average Pb−O bond length in $CaPbO_3$ was virtually the same as that in $SrPbO_3$ (i.e., 2.161 Å[5]). This average length is slightly larger than 2.149 Å in $BaPbO_3$[5] despite the larger ionic radius of Ba^{2+} than those of Ca^{2+} and Sr^{2+}. On the other hand, PbO_6 octahedra are appreciably tilted with each other, as can be appreciated from Figure 5b. Various geometrical parameters evidently reveal that $CaPbO_3$, and to a lesser extent $SrPbO_3$, is structurally distorted. Tilt angles around $[001]_p$ and $[110]_p$ axes (p: perovskite subcell) are, respectively, 20.28(4)° and 18.50(3)° in $CaPbO_3$, and 11° and 15.1° in $SrPbO_3$.[5] In the case of $BaPbO_3$ with higher symmetry, each PbO_6 octahedron tilts only around the $[110]_p$ axis by a much smaller angle of 8.4°.[5] The more pronounced tilts in $CaPbO_3$ than those in $SrPbO_3$ and $BaPbO_3$ are indispensable for forming coordination polyhedra favorable for small Ca^{2+} ions.

The bond-valence sums of Ca and Pb in $CaPbO_3$ were calculated from bond lengths in Table 4 according to a procedure proposed by Brown and Altermatt.[26] The bond-valence sums were estimated at +1.70 for Ca and +4.34 for Pb, whereas those in Ca_2PbO_4[19] at +1.97 for Ca and +4.04 for Pb. Such large deviations of the oxidation states from the ideal ones are common to perovskite-type $APbO_3$ (A = Ca, Sr and Ba),[5,10] which may reflect considerable covalent character conceded in these lead(IV) oxides, particularly in their Pb−O bonds.[27] It should, however, be pointed out that the marked tilts of PbO_6 octahedra already described may be a more important factor ruling the labilization of perovskite-type $CaPbO_3$ relative to Ca_2PbO_4 under ambient pressure.

Chemical Stability and Electrical Properties of $CaPbO_3$. Figure 6 shows the relative weight change of $CaPbO_3$ during heating and subsequent cooling processes. Hardly any weight change was detected below 550 °C. Above 700 °C, about 2.5% of weight loss corresponding 0.5 oxygen per formula unit were ob-

(26) Brown, I. D.; Altermatt, D. *Acta Crystallogr.* **1985**, *41B*, 244.
(27) Müller, U. In *Inorganic Structural Chemistry*; Wiley: Chichester, 1993; p 35.

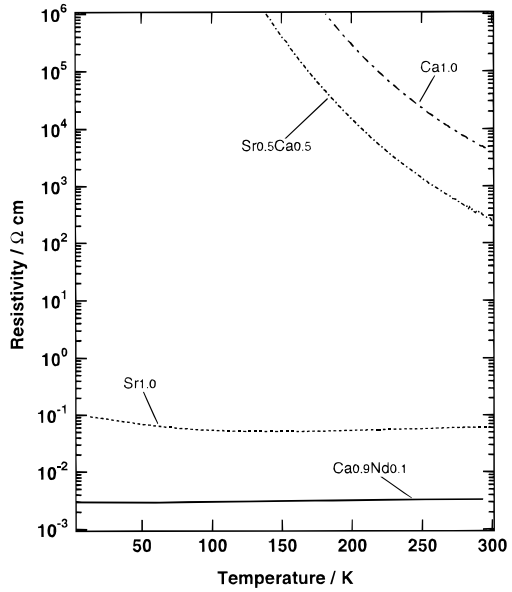

Figure 7. Dependence of electrical resistivities for $Ca_{1-x}Sr_x$-PbO_3 ($x = 0$, 0.5, and 1) and $Ca_{0.9}Nd_{0.1}PbO_3$ on temperature.

served, and the weight never returned to the initial level after cooling. The XRD analysis of a cooled sample showed that the reduction in weight is caused by decomposition of $CaPbO_3$ into Ca_2PbO_4 and PbO with liberation of O_2:

$$2CaPbO_3 \rightarrow Ca_2PbO_4 + PbO + 1/2O_2$$

In the course of the heating and cooling up to 550 °C, no weight changes occurred. The TGA of $CaPbO_3$ clearly revealed that perovskite-type $CaPbO_3$ is not stable above 550 °C, which is in good agreement with the temperature of decomposition for another polymorph of $CaPbO_3$.[13] The thermal decomposition of $CaPbO_3$ at temperatures exceeding 550 °C is associated with the high stability of Ca_2PbO_4 at high temperature as already described.

As Figure 7 illustrates, the resistivity of $CaPbO_3$ at room temperature was as high as $\approx 3 \times 10^3$ Ω•cm, and logarithmically increased with lowering temperature down to 180 K. Resistivities at temperatures $\ll$180 K were too high to determine them accurately with our experimental apparatus. Such low conductivity forms a striking contrast with metallic conductivity in $BaPbO_3$[1] and $SrPbO_3$.[7] The gap energy, E_g, estimated by assuming thermal-activation-type conduction was 0.43 eV.

The band structure of $CaPbO_3$ is believed to be similar to those of $BaPbO_3$ and $SrPbO_3$ [5,10] because of their structural similarity. The large deviation of the O−Pb−O bond angles from 90° reduces the degree of overlapping of the 6s(Pb) and 2p(O) orbitals.[5] The O−Pb−O bond angles in $CaPbO_3$ and $SrPbO_3$ given in Table 4 and those in $BaPbO_3$ (90.4° and 90.96°)[5] offer conclusive evidence for the idea that this deviation increases with decreasing ionic radius of A^{2+}. Hence, poorly overlapping orbitals must be induced in $SrPbO_3$ and particularly $CaPbO_3$ by the marked tilting of the PbO_6 octahedra, in other words, bending of Pb−O−Pb bonds in the three-dimensional network of corner-sharing PbO_6 octahedra. We should also note possible influences of the alkaline earth metals on the covelent character of Pb−O bonds. Ca, and to a lesser extent Sr, will reduce the covalency of the Pb−O bonds because of their electronegativites (1.00 for Ca and 0.95 for Sr) higher than that of Ba (0.89),[28] which would narrow the 6s(Pb)-2p(O) spσ band to widen the energy gap between the nonbonding and antibonding bands. These ideas are in harmony with the experimental facts that the electric resistivity in $APbO_3$ (A = Ca, Sr, and Ba) decreases with increasing size of A^{2+}.

Changes in Structure and Electrical Properties on Substitutions at A sites. We investigated Ca_{1-x}-Sr_xPbO_3 ($x = 0.5$ and 1) and $CdPbO_3$ with the aim of exploring size effects of A-site metals on structure and conductivity. Table 5 lists their lattice parameters, orthorhombic lattice strains, $e = 2(b - a)/(b + a)$, and unit-cell volumes, V, determined by XRD. The samples of $Ca_{1-x}Sr_xPbO_3$ were obtained without any impurity by reaction at 1000 °C and 5 GPa for 1 h. With increasing Sr content, lattice parameters increased while e, which is a measure of structural distortion, decreased considerably. $Ca_{1-x}Sr_xPbO_3$ could occur only under high pressure, whereas Ca_2PbO_4 was preferentially formed under ambient pressure. We did not find any noticeable difference between lattice parameters of $SrPbO_3$ samples synthesized under ambient and high pressure. Figure 7 shows the dependence of electrical resistivity for $Ca_{1-x}Sr_xPbO_3$ on temperature. The resistivity of $Ca_{0.5}$-$Sr_{0.5}PbO_3$ was $\approx 2 \times 10^2$ Ω•cm at room temperature and logarithmically increased with lowering temperature at least down to 140 K, which suggests gap formation similar to that in $CaPbO_3$. An estimated gap energy of 0.36 eV smaller than that for $CaPbO_3$ is ascribed to the reduction in the distortion. On the other hand, the resistivity of $SrPbO_3$ was of 10^{-2} Ω•cm order. Its temperature dependence exhibited metallic character although an upturn was observed at low temperature; the reason for the upturn was discussed by Lobanov et al.[7] The decrease in e with increasing Sr content seems to cause the decrease in the gap width.

The Cd^{2+} ion possesses roughly the same effective ionic radius, r, as the Ca^{2+} ion: $r(Cd^{2+}) = 1.10$ Å and $r(Ca^{2+}) = 1.12$ Å for 8-fold coordination.[29] Perovskite-type $CdPbO_3$ was formed along with Cd_2PbO_4 regardless of the synthetic routes. The perovskite-type compound was obtainable from CdO and PbO_2 with concomitant formation of small amounts of impurity phases including Cd_2PbO_4. The SEM-EDX analysis showed the main phase to be nearly stoichiometric $CdPbO_3$. Kudo et al.[30] also attempted to prepare $CdPbO_3$ by reaction at 700 °C under 7.5 GPa for 30 min, but the product included Cd_2PbO_4 as an impurity. Though resistivity measurements suggested the insulating behavior of perovskite-type $CdPbO_3$, further work is required to get single-phase $CdPbO_3$ and study its crystal structure and properties.

The negligibly small amounts of oxygen and substitutional defects in $CaPbO_3$ will lead to an almost empty antibonding band. Then, we substituted R^{3+} ions (R = La, Nd, and Y) for Ca^{2+} ions to introduce electron carriers into the antibonding band (Table 5). The

(28) Shriver, D. F.; Atkins, P. W.; Langford, C. H. In *Inorganic Chemistry*, 2nd Ed.; Oxford University Press: Oxford, 1994; p 44.
(29) Shannon, R. D. *Acta Crystallogr.* **1976**, *32A*, 751.
(30) Kudo, N.; Syono, Y.; Kusaba, K.; Kikuchi, M., unpublished data.

Table 5. Lattice Parameters, Orthorhombic Lattice Strain, and Unit-Cell Volumes of $Ca_{1-x}A_xPbO_3$ (A = Sr and Cd) and $Ca_{1-x}R_xPbO_3$ (R = La, Nd and Y)

nominal composition	*a*, Å	*b*, Å	*c*, Å	*e*	*V*, Å^3	impurities
$CaPbO_3$	5.661(1)	5.878(1)	8.136(1)	0.0376	270.7(1)	none
$Ca_{0.5}Sr_{0.5}PbO_3$	5.780(2)	5.931(2)	8.260(2)	0.0258	283.1(3)	none
$SrPbO_3$	5.854(1)	5.950(1)	8.318(1)	0.0084	289.7(1)	none
$CdPbO_3$	5.676(1)	5.869(1)	8.153(2)	0.0334	271.6(1)	Cd_2PbO_4
$Ca_{0.9}La_{0.1}PbO_3$	5.694(1)	5.906(1)	8.191(2)	0.0366	275.5(1)	none
$Ca_{0.8}La_{0.2}PbO_3$	5.729(1)	5.930(1)	8.239(1)	0.0344	279.9(1)	unknown
$Ca_{0.9}Nd_{0.1}PbO_3$	5.681(1)	5.897(1)	8.174(2)	0.0374	273.9(1)	trace
$Ca_{0.9}Y_{0.1}PbO_3$	5.670(1)	5.891(1)	8.159(1)	0.0382	272.6(1)	trace

solubility range in $Ca_{1-x}La_xPbO_3$ was $x = 0.1-0.2$ under our experimental conditions. When doping Nd^{3+} (r = 1.11 Å) and Y^{3+} (r = 1.02 Å) whose ionic radii are smaller than that of La (r = 1.16 Å),[29] solubility limits were almost the same as that in $Ca_{1-x}La_xPbO_3$. Table 5 shows that the lattice parameters and e of $Ca_{1-x}R_xPbO_3$ respectively decreased and increased with decreasing $r(R^{3+})$. The resistivities of the R-doped samples were metallic in marked contrast with undoped $CaPbO_3$ despite slight changes in structural distortion because of $r(R^{3+})$ comparable to $r(Ca^{2+})$. Figure 7 exemplifies a plot of resistivity versus temperature curve for $Ca_{0.9}Nd_{0.1}PbO_3$ which possesses almost the same e value as does $CaPbO_3$. Carrier doping into the empty antibonding band must be responsible for such metallic properties. These experimental facts, coupled with $r(R^{3+})$ similar to $r(Ca^{2+})$, show that the conductivities of the perovskites based on $APbO_3$ are governed not only by structural distortion accompanying the gap formation but by doping of electron carriers in the unoccupied band. Details of the crystal structures and transport properties including thermoelectric power for $A_{1-x}La_xPbO_3$ (A = Ba, Sr, and Ca) will be reported elsewhere.[11,31]

Summary

The reaction of the Ca_2PbO_4 precursor with PbO_2 under high pressure afforded $CaPbO_3$ of high purity. This orthorhombic form of $CaPbO_3$ is crystal chemically isotypic to $SrPbO_3$ with the distorted perovskite-type structure of the $GdFeO_3$ type. Neither oxygen deficiencies nor substitutional defects could be detected by Rietveld refinement of the neutron diffraction data on the basis of space group Pbnm. Distortion from the ideal cubic perovskite-type structure was much more pronounced in $CaPbO_3$ than in $BaPbO_3$ or $SrPbO_3$, owing to the smaller ionic radius of the Ca^{2+} ion. The PbO_6 octahedra are almost regular but considerably tilted with each other with tilt angles around $[001]_p$ and $[110]_p$ as large as 20.28° and 18.50°, respectively. Unlike $BaPbO_3$ and $SrPbO_3$ exhibiting metallic conductivity, the electric resistivity of $CaPbO_3$ at room-temperature amounted to 3×10^3 Ω•cm. Such insulating behavior of $CaPbO_3$ is ascribable to the presence of the gap between the 2p(O) nonbonding band and the 6s(Pb)-2p(O) spσ antibonding band. The energy gap, which is missing in $BaPbO_3$, is believed to arise from the decrease in the overlap of the 6s(Pb) and 2p(O) orbitals as a result of the marked structural distortion and possibly from the increase in the covalency of the Pb−O bonds. We demonstrated that partial substitution of trivalent cations for Ca^{2+} ions dramatically decreases resistivity through introduction of electron carriers into the unoccupied band. This doping method hardly causes changes in the conduction path; that is, the three-dimensional network of PbO_6 octahedra. Its application to the metallization of other lead(IV) oxides with layer and/or network structures containing PbO_6 octahedra could give rise to interesting physical properties including superconductivity.

Acknowledgment. We thank Y. Syono of Tohoku University for helpful discussions and T. Ikeda of the University of Tsukuba for help in the structure refinement. This work was partly supported by NEDO. Figure 5 was produced with ATOMS 4.1 by Shape Software.

CM980629P

(31) Yamamoto, A.; Ono, T.; Tatsuki, T.; Tamura, T.; Tajima, S. *Materials Res. Bull.*, In press.